BIOCHEMISTRY
including biophysical chemistry & molecular biology

Article

pubs.acs.org/biochemistry

Relationship of the Topological Distances and Activities between mPGES-1 and COX-2 versus COX-1: Implications of the Different Post-Translational Endoplasmic Reticulum Organizations of COX-1 and COX-2

Hironari Akasaka, Shui-Ping So, and Ke-He Ruan*

Department of Pharmacological and Pharmaceutical Sciences, Center for Experimental Therapeutics and Pharmacoinformatics, College of Pharmacy, University of Houston, Houston, Texas 77204-5037, United States

ABSTRACT: In vascular inflammation, prostaglandin E2 (PGE_2) is largely biosynthesized by microsomal PGE_2 synthase-1 (mPGES-1), competing with other downstream eicosanoid-synthesizing enzymes, such as PGIS, a synthase of a vascular protector prostacyclin (PGI_2), to isomerize the cyclooxygenase (COX)-2-derived prostaglandin H2 (PGH_2). In this study, we found that a majority of the product from the cells co-expressing human COX-2, mPGES-1, and PGIS was PGE_2. We hypothesize that the molecular and cellular mechanisms are related to the post-translational endoplasmic reticulum (ER) arrangement of those enzymes. A set of fusion enzymes, COX-2-linker [10 amino acids (aa)]-PGIS and COX-2-linker (22 amino acids)-PGIS, were created as "The Bioruler", in which the 10 and 22 amino acids are defined linkers with known helical structures and distances (14.4 and 30.8 Å, respectively). Our experiments have shown that the efficiency of PGI_2 biosynthesis was reduced when the separation distance increased from 10 to 22 amino acids. When COX-2-10aa-PGIS (with a 14.4 Å separation) was co-expressed with mPGES-1 on the ER membrane, a major product was PGE_2, but not PGI_2. However, expression of COX-2-10aa-PGIS and mPGES-1 on a separated ER with a distance of ≫30.8 Å reduced the level of PGE_2 production. These data indicated that the mPGES-1 is "complex-likely" colocalized with COX-2 within a distance of 14.4 Å. In addition, the cells co-expressing COX-1-10aa-PGIS and mPGES-1 produced PGI_2 mainly, but not PGE_2. This indicates that mPGES-1 is expressed much farther from COX-1. These findings have led to proposed models showing the different post-translational ER organization between COX-2 and COX-1 with respect to the topological arrangement of the mPGES-1 during vascular inflammation.

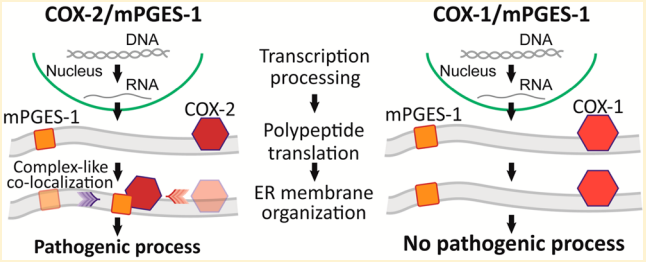

Vascular inflammation is a serious pathogenic factor that underlies the development of atherosclerosis, arterial aneurisms, and other cardiovascular diseases. If prolonged, it could rupture vascular walls or vascular tissues, resulting in one of the highest rates of morbidity and mortality. Cyclooxygenase-1 (COX-1) and cyclooxygenase-2 (COX-2) play an important role in physiological and inflammatory events by mediating the production of active lipid metabolites known as prostaglandins (PGs).[1] The pathway is initiated by the release of arachidonic acid (AA) from phospholipids. AA is then catalyzed by COX-1 and COX-2 into the unstable endoperoxide, prostaglandin H2 (PGH_2). PGH_2 is a common substrate, passed to various terminal prostaglandin synthases (PGSs), synthesizing their respective products (PGD_2, PGE_2, PGF_2, PGI_2, and TXA_2). Within PGs, PGI_2 biosynthesized by PGI_2 synthase (PGIS) in endothelial cells contributes to potent cardiovascular protection by vasodilation and anticoagulation.[2] PGE_2 is involved in physiological events in basal amounts, but it also plays a role in the development of vascular inflammatory diseases when the amounts are excessive.[1] A basal amount of PGE_2 is constitutively biosynthesized by COX-1, cytosolic PGE_2 synthase (cPGES), and microsomal PGES-2 (mPGES-2). An excess of PGE_2 is biosynthesized by COX-2 and mPGES-1.[3] COX-2 and mPGES-1 are induced in response to inflammatory stimuli, growth factors, and hormones, contributing to pain, fever, and inflammation. In vascular inflammation, PGE_2 is largely biosynthesized by mPGES-1 in competition with PGIS in endothelial cells.[4] The molecular and cellular mechanisms involved to encourage synthesis of inflammatory PGE_2 over synthesis of other eicosanoids (such as PGI_2) during the inflammatory process are not clearly understood. COX-2, mPGES-1, and PGIS are expressed in the perinuclear envelope and endoplasmic reticulum (ER).[4−7] In addition, both mPGES-1 and PGIS can utilize a COX-2-derived substrate, PGH_2.[6,8] To determine how COX-2 and mPGES-1 produce a disproportionately large amount of PGE_2 in inflammation, we designed an experiment to determine the cellular environment of COX-2, mPGES-1, and PGIS using our fusion enzymes, which have a defined distance (10 or 22 amino acids) and orientation

Received: March 31, 2015
Revised: May 14, 2015
Published: May 19, 2015

DOI: 10.1021/acs.biochem.5b00339
Biochemistry 2015, 54, 3707−3715

between COXs and PGIS. The fusion enzymes were engineered on the basis of structural and functional characterizations of the coupling between COXs and its downstream enzymes, including PGIS. On the basis of the structural information, the COX-2-10aa-PGIS fusion enzyme,[9] which links COX-2 to PGIS through a helical transmembrane (TM) segment consisting of 10 residues, was first engineered. The hybrid enzymes not only adopted the three catalytic functions of the parent COX-2 and PGIS (AA to PGG_2, PGG_2 to PGH_2, and PGH_2 to PGI_2) but also increased the initial velocity of the enzyme reactions, resulting in faster and more specific production of PGI_2.[9,10] These fusion enzymes allow us to test the effects of the topological arrangements between COX-2 and mPGES-1 or PGIS on the production of PGE_2 in ER membranes. This study has found a complexlike colocalization between COX-2 and mPGES-1 over a short distance of approximately 14.4 Å, which is the fundamental reason to have mPGES-1 catching PGH_2 from COX-2 and then converting it to PGE_2 effectively.

MATERIALS AND METHODS

Materials. The HEK293 cell line was purchased from ATCC (Manassas, VA). Dulbecco's modified Eagle's medium for culturing the cell lines and lipofectamine 2000 for transfecting cDNAs were purchased from Invitrogen (Carlsbad, CA). [^{14}C]AA was purchased from PerkinElmer (Waltham, MA). The primary antibodies for human COX-2, mPGES-1, and PGIS were purchased from Cayman Chemical Co. (Ann Armor, MI).

Cell Culture. HEK293 cells were cultured in a 100 mm cell culture dish with high-glucose Dulbecco's modified Eagle's medium containing 10% fetal bovine serum and antibiotic and antimycotic and grown at 37 °C in a humidified 5% CO_2 incubator.

Construction of COX and PG Synthase Expression Vectors. The cDNA of the engineered TriCat enzymes (COX-2-10aa-PGIS and COX-2-22aa-PGIS) was previously described.[9] Briefly, COX-2 was linked to a 10-amino acid (aa) or 22 aa transmembrane linker connected to PGIS. COX-2 was generated by a polymerase chain reaction approach and then subcloned into a pcDNA3.1 vector with a cytomegalovirus early promoter. The resultant pcDNA3.1-COX-2-10aa-PGIS was used for expressing the TriCat enzymes in HEK293.

Expression of COX-10aa-PGIS and mPGES-1 in HEK293 Cells. The recombinant synthases (COX-2-10aa-PGIS and COX-1-10aa-PGIS) were expressed in HEK293 cells. Briefly, the cells were grown and transfected with the purified cDNA of the recombinant protein by the Lipofectamine 2000 method, following the manufacturer's instructions (Invitrogen). For transient expression, approximately 48 h after transfection, the cells were harvested for further enzyme assays and a Western blot analysis was performed. For stable expression, the transfected cells were incubated with culture medium containing Geneticin (G418).

Determination of Enzyme Activity for PGIS and mPGES-1 Using High-Performance Liquid Chromatography (HPLC). To determine the activity of the synthases that converted AA into PGI_2 through PGIS or PGE_2 through mPGES-1, [^{14}C]AA was added to the harvested cells in a total reaction volume of 0.1 mL. After incubation for 5 min, the reaction was stopped by adding 0.2 mL of buffer A (containing 0.1% acetic acid and 30% acetonitrile). After centrifugation (13000 rpm for 10 min), the supernatant was collected and loaded onto a reverse phase C18 column (Varian Microsorb-MV 100-5, 4.6 mm × 250 mm) using the buffer A with a gradient from 35 to 100% of acetonitrile for 40 min with a flow rate 1.0 mL/min. The metabolized [^{14}C]AA in the end product profile was monitored directly by a flow scintillation analyzer (Packard 150TR).

Immunoblot Analysis. The cultured cells were collected and washed with PBS. The proteins were separated by 7 to 10% (w/v) sodium dodecyl sulfate–polyacrylamide gel electrophoresis under denaturing conditions and then transferred to a nitrocellulose membrane. Bands recognized by individual primary antibodies were visualized with horseradish peroxidase-conjugated secondary antibodies.

Statistic. Statistical significance was shown as the mean ± the standard deviation using Origin9. A t test was used to compare two groups. $p < 0.05$ was considered significant.

RESULTS

Identification of mPGES-1 Played a Key Role in Redirecting Endogenous AA to Pathogenic PGE_2 Biosynthesis in the ER Membrane. During inflammation, COX-2 and mPGES-1 are induced to redirect the endogenous AA metabolite from the balanced prostanoid biosyntheses to the unbalanced conditions, in which inflammatory PGE_2 is overproduced and the extents of biosynthesis of other prostanoids, such as TXA_2 and PGI_2, were reduced.[11,12] To see how a large amount of PGE_2 can be produced by the induced COX-2 coordinating with mPGES-1, we created recombinant HEK293 cells stably expressing COX-2 and mPGES-1 [HEK293-COX-2/mPGES-1 (Figure 1A, lane 1)][13] to mimic the inflammatory condition. Using a trace amount of [^{14}C]AA to monitor the endogenous AA metabolite in the cells, HEK293-COX-2/mPGES-1 completely directed the AA metabolite to PGE_2 (Figure 1B). To see whether the noninducible cPGES and mPGES-2 in the HEK293 cells were also involved in the PGE_2 biosynthesis for the HEK293-COX-2/mPGES-1 cells, the HEK293 cells were transfected with COX-2 only [HEK293-COX-2 (Figure 1A, lane 2)] and then monitored for endogenous AA metabolites. Very little PGE_2, but a large amount of $PGF_{2\alpha}$ (product of the nonenzymatic degradation of COX-2-derived PGH_2), was produced by the HEK293-COX-2 cells (Figure 1C). In contrast, [^{14}C]AA was not metabolized in the HEK293 cells expressing only mPGES-1 (Figure 1A, lane 3, and Figure 1D) or the HEK293 control cells (Figure 1A, lane 4, and Figure 1E). This demonstrated that PGH_2 produced by COX-2 was effectively and completely presented to mPGES-1 to be used for PGE_2 production under the mimicked inflammatory cells (Figure 1B) but was very ineffectively presented to cPGES and mPGES-2 to be converted into PGE_2 (Figure 1C). Similarly, in the absence of COX-2, inducible mPGES-1 does not have the ability to metabolize AA to PGE_2 (Figure 1D). This led to the conclusion that COX-2 alone would not cause too much PGE_2-mediated inflammation, and mPGES-1 alone does not have the ability to mediate inflammation. However, the presence of inducible mPGES-1 and COX-2 creates a powerful inflammatory system, converting almost all AA into inflammatory PGE_2 compared to COX-2 only, whereby approximately 15% of AA was converted into PGE_2, to advance the inflammation. Thus, inhibiting mPGES-1 could be an important approach for treating inflammation. It also raises the questions of why and how the inducible mPGES-1 coordinated with COX-2 is so much more effective than noninducible cPGES and mPGES-2,

DOI: 10.1021/acs.biochem.5b00339
Biochemistry 2015, 54, 3707–3715

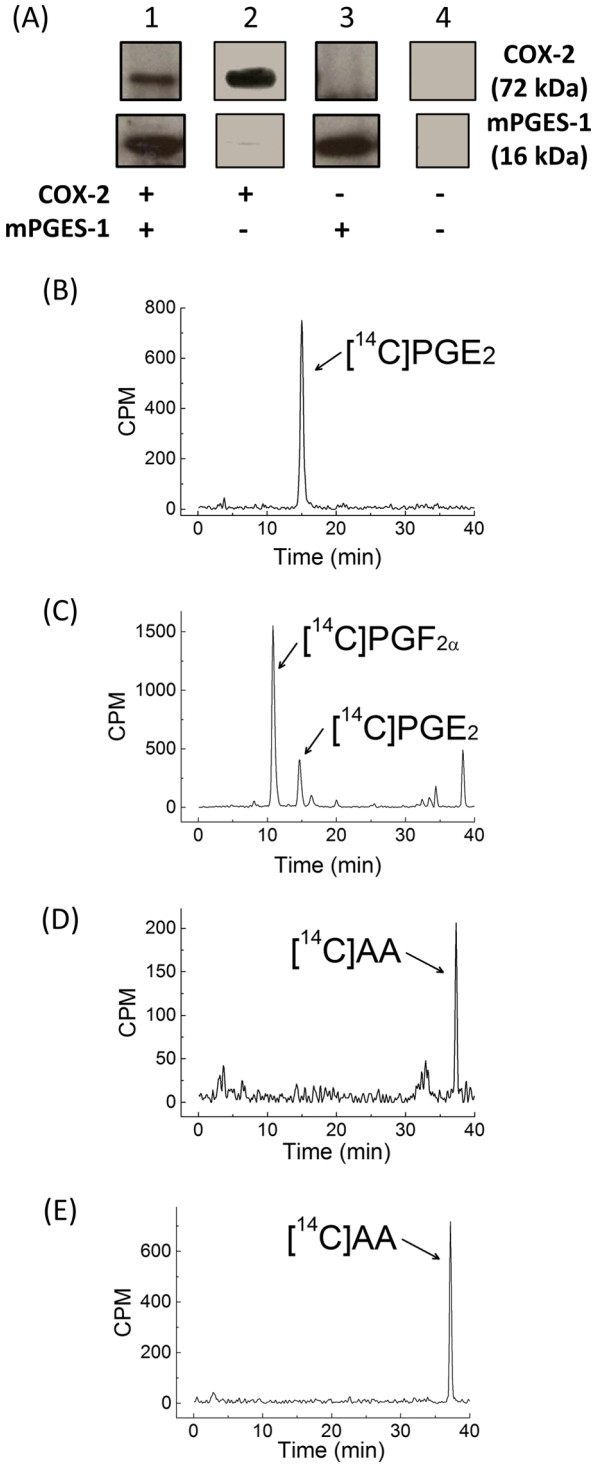

Figure 1. (A) Western blot analysis of the HEK293 cells transfected with the cDNA(s) of COX-2 and mPGES-1 (lane 1), COX-2 only (lane 2), and mPGES-1 only (lane 3). Lane 4 contained control HEK293 cells transfected with vector only. The antibodies used for analysis were a mixture of monoclonal mouse anti-human COX-2 and mPGES-1 antibodies. Full profiles of the incorporated [^{14}C]AA metabolite made by the HEK293 cells expressing (B) COX-2 and mPGES-1, (C) COX-2 only, (D) mPGES-1 only, and (E) vector control protein only.

and even that of other noninducible prostanoid synthases, such as PGIS and TXAS, in which those enzymes anchored to the ER membrane like mPGES-1 shared PGH_2 as their substrates for TXA_2 and PGI_2 production. Understanding the molecular and cellular mechanisms behind how mPGES-1 effectively accepts PGH_2 from COX-2 in the ER membrane environment to redirect the AA metabolite to PGE_2 is a key step toward addressing these questions and toward designing a specific inhibitor against inflammation to replace the COX-2 inhibitor that has the potential to cause cardiovascular damage.

Testing the Competition of mPGES-1 and PGIS To Accept PGH_2 from COX-2 in the ER Lipid Bilayers. The stable cell line expressing COX-2 and mPGES-1 was transfected with PGIS cDNA to generate a cell line triply co-expressing COX-2, mPGES-1, and PGIS (HEK293-COX-2/mPGES-1/PGIS). The majority of the [^{14}C]AA metabolite was [^{14}C]PGE_2, but not PGI_2 (Figure 2A). To determine the

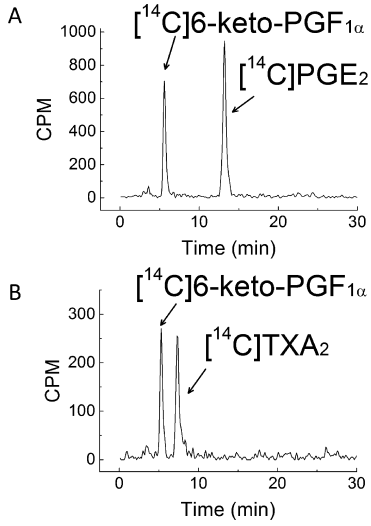

Figure 2. Full profiles of the incorporated [^{14}C]AA metabolite made by the HEK293 cells expressing (A) COX-2, mPGES-1, and PGIS and (B) COX-2, mPGES-1, and TXAS.

product distribution for the other co-expression of COX-2 downstrean enzymes, HEK293 cells co-expressing COX-2, PGIS, and TXAS were created. PGI_2 and TXA_2 were equally produced (Figure 2B). This demonstrates that mPGES-1 has a higher priority to take PGH_2 from COX-2 than that of PGIS in the ER lipid bilayers. The co-expressed TXAS has an ability identical to that of PGIS to share the COX-2-derived PGH_2. It implies that in the presence of mPGES-1 in the inflammatory tissues and cells, the possibility of developing endothelial dysfunction and heart diseases is likely determined by the fact that mPGES-1 has an ability to catch PGH_2 from COX-2 faster and stronger than that of PGIS and therefore produces a larger amount of PGE_2 and a smaller amount of PGI_2 (Figure 2A).

Characterization of the Molecular and Cellular Mechanisms of mPGES-1 Having a Priority of Catching COX-2-Derived PGH_2 That Is Higher Than That of Other Downstream Enzymes (K_m comparison). We focused on one of the downstream enzymes, PGIS, as an example for comparison with mPGES-1 in catching COX-2-derived PGH_2. By comparison of the K_m values using PGH_2 as a common substrate, PGIS and mPGES-1 revealed very similar patterns. The K_m values are in the lower micromolar range,[9,13] which is not a significant difference. This has led us to consider other factors besides the affinities of the substrate for both enzymes.

Determination of the Topological Factors That Affect mPGES-1 as It Catches COX-2-Derived PGH_2, Having a

DOI: 10.1021/acs.biochem.5b00339
Biochemistry 2015, 54, 3707−3715

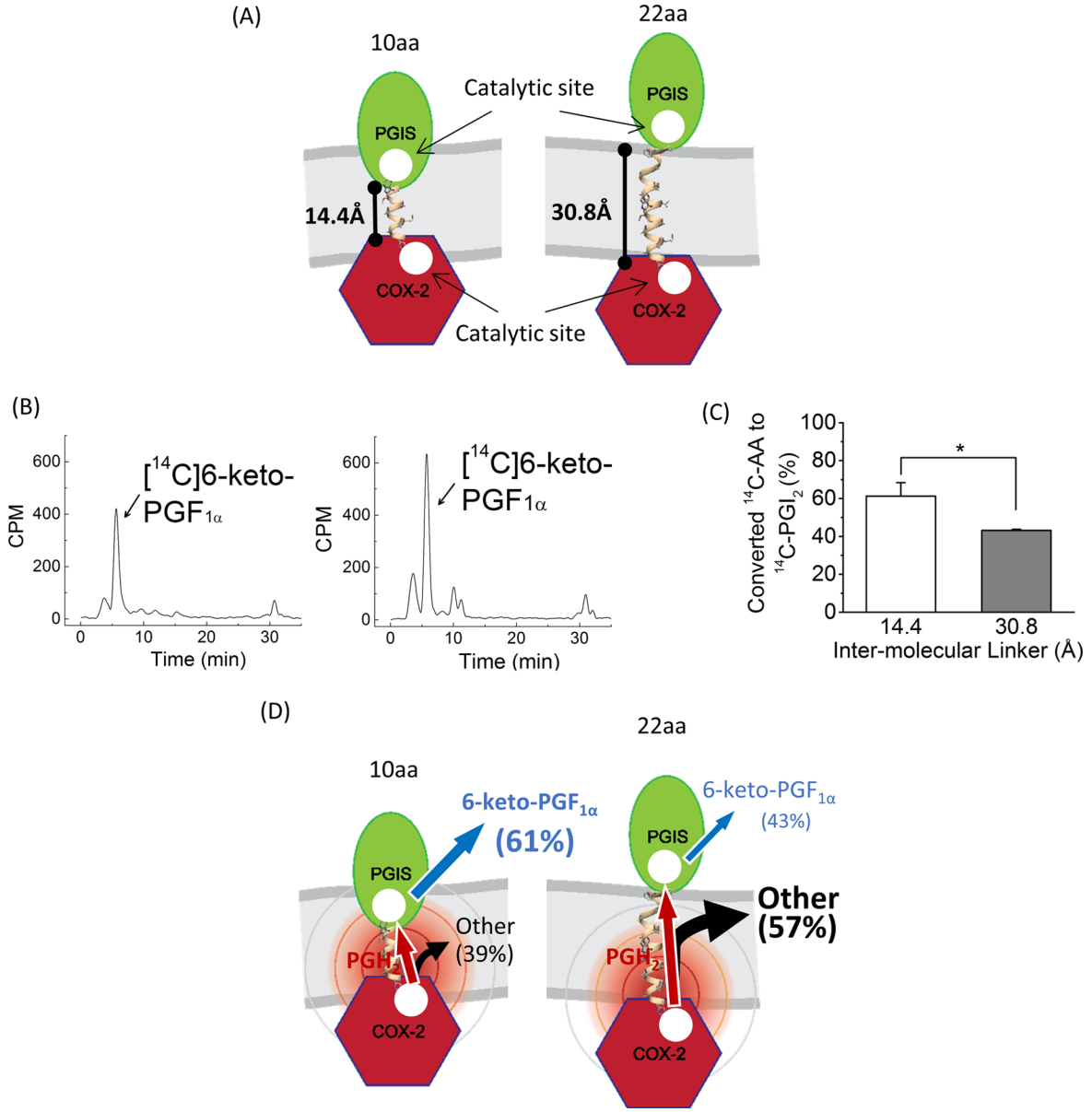

Figure 3. (A) Comparison of the structural and topological differences between the hybrid enzymes linking COX-2 and PGIS with 10 (left) or 22 aa (right). (B) Full profiles of the incorporated [^{14}C]AA metabolite made by the HEK293 cells expressing COX-2 and PGIS with 10 (left) or 22 aa (right). (C) Determination of the catalytic activity based on their linker lengths. The percentages for the [^{14}C]AA converted to [^{14}C]PGI2 were calculated using the area under the curve of the peaks ($p < 0.05$). (D) Putative models of the relationship between PGI2 synthesis and the distance between COX-2 and PGIS.

Rate Higher Than That with PGIS in ER Lipid Bilayers. COX-2 and its downstream enzymes, such as PGIS, TXAS, mPGES-1, and mPGES-2, are all synthesized in the ER, organized into 3D structures, and anchored to ER lipid bilayers to coordinate the prostanoid biosyntheses. It is known that PGH_2 synthesized and then released by COX-2 is hydrophobic and freely moving within ER lipid bilayers at a very rapid speed. Thus, we hypothesized that the distance between COX-2 and mPGES-1 and other downstream synthases could be one of the key factors determining the priority of catching PGH_2 for different prostanoid biosyntheses. To test this hypothesis, we used "The Bioruler", which has a defined distance between COX and PGIS as a reference and predicts an unknown distance between COX and another downstream synthase, such as mPGES-1 in the ER lipid bilayers.

Determination of the Relationship of the Distance between COX-2 and PGIS and the Ability To Catch PGH_2 Using "The Bioruler", COX-2-Linker-PGIS, as a Reference. We used the previously engineered active fusion enzymes, COX-2-linker-PGIS, which linked COX-2 with PGIS through defined linkers with the known lengths of 10 or 22 aa.[9] These linkers are adopted from known 3D helical structures of the transmembrane domain of human rhodopsin. The distances for the separations of the helical 10 and 22 aa linkers spanning the ER membrane are 14.4 Å (Figure 3A, left) and 30.8 Å (Figure 3A, right), respectively. Expressing the fusion enzymes in the HEK293 cells, they adopt the ER topological arrangement and triple catalytic activities of COX-2 and PGIS to continually convert AA to PGG_2, PGH_2, and then PGI_2 within a single polypeptide.[9] One of the rates determining PGI_2 production is based on how fast the PGIS domain can

DOI: 10.1021/acs.biochem.5b00339
Biochemistry 2015, 54, 3707−3715

catch the COX-2 domain-derived PGH_2 within the limited distance before the degradation of PGH_2 that diffused into the ER environment (Figure 3A). The relationship between the distance from COX-2 to PGIS, which affects the concentration of PGH_2 reaching PGIS and PGI_2 production, was measured by comparing the yield of PGH_2 converted to PGI_2 and its degraded side products using specific [^{14}C]AA metabolite profiling. The fusion enzyme with a longer linker distance of 30.8 Å, 22 aa (Figure 3B, right), has more side products than that with a linker distance of 14.4 Å, 10 aa (Figure 3B, left). The relationship of the intermolecular distance between the COX-2 domain and PGIS domain within the fusion enzymes and the yield of PGI_2 production is plotted in Figure 3C. The results show that the distance between COX-2 and PGIS affected PGH_2 moving from the COX-2 domain to the PGIS domain in the fusion enzymes. The longer distance caused the loss of more PGH_2 during the movement from the COX-2 domain to the PGIS domain (Figure 3D).

Prediction of the Separation Distance between COX-2 and mPGES-1 with Respect to the ER Membrane. The concept and observation described above were used to predict the unknown distance between COX-2 and mPGES-1 in the ER membrane because PGH_2 moved from COX-2 to mPGES-1 in a similar manner by a diffusion mechanism, and both PGIS and mPGES-1 are anchored to the ER membrane near COX-2. When we co-expressed COX-2-10aa-PGIS with mPGES-1, the movement of COX-2-derived PGH_2 to mPGES-1 or PGIS was based on distance (Figure 4A). Interestingly, the majority of PGH_2 moved to the mPGES-1 pocket and was converted into PGE_2 (Figure 4B), including even PGIS with a distance from COX-2 of only 14.4 Å within the fusion enzyme (Figure 4B). In contrast, in the absence of mPGES-1, PGH_2 was almost 100% moved to the PGIS domain and converted to PGI_2 by the fusion enzyme (Figure 3B, left). These data demonstrate that the mPGES-1 binding pocket is <14.4 Å from the COX-2 domain, catching more than 85% of the PGH_2 from the COX-2 domain (Figure 4C). This important finding has allowed us to uncover the cellular and molecular mechanisms of how induced mPGES-1 has the priority to catch COX-2-derived PGH_2, redirecting endogenous AA toward the production of pathogenic PGE_2 in a high-efficiency and high-yield manner (Figure 4C). It also raises the possibility of the complexlike colocalization of COX-2 and mPGES-1 in the ER membrane through molecule−molecule interaction during inflammatory stimulation because the predicted distance is as short as <14.4 Å.

Comparison of PGH_2 Moved from COXs to mPGES-1 in the Non-Inflammatory Condition. Compared to COX-2 as an inducible and inflammatory marker enzyme, COX-1 is a housekeeping and non-inflammatory COX isoenzyme. To rule out the possibility that mPGES-1 might have an affinity for PGH_2 higher than that of PGIS (lower K_m value), we replaced the COX-2-10aa-PGIS using COX-1-10aa-PGIS co-expressed with mPGES-1 in the HEK293 cells [HEK293-COX-1-10aa-PGIS/mPGES-1 (Figure 5A)]. Interestingly, COX-1-derived PGH_2 was largely converted to PGI_2, but a very small amount was converted to PGE_2 (Figure 5B). This finding clearly ruled out the possibility that mPGES-1 has an affinity for PGH_2 higher than that of PGIS. This was further ruled out by the model described above, in which the short distance (<14.4 Å) between COX and mPGES-1 determines the priority for mPGES-1 to take PGH_2 for biosynthesizing PGE_2 competing with PGIS with a distance of 14.4 Å (Figure 4C). The finding

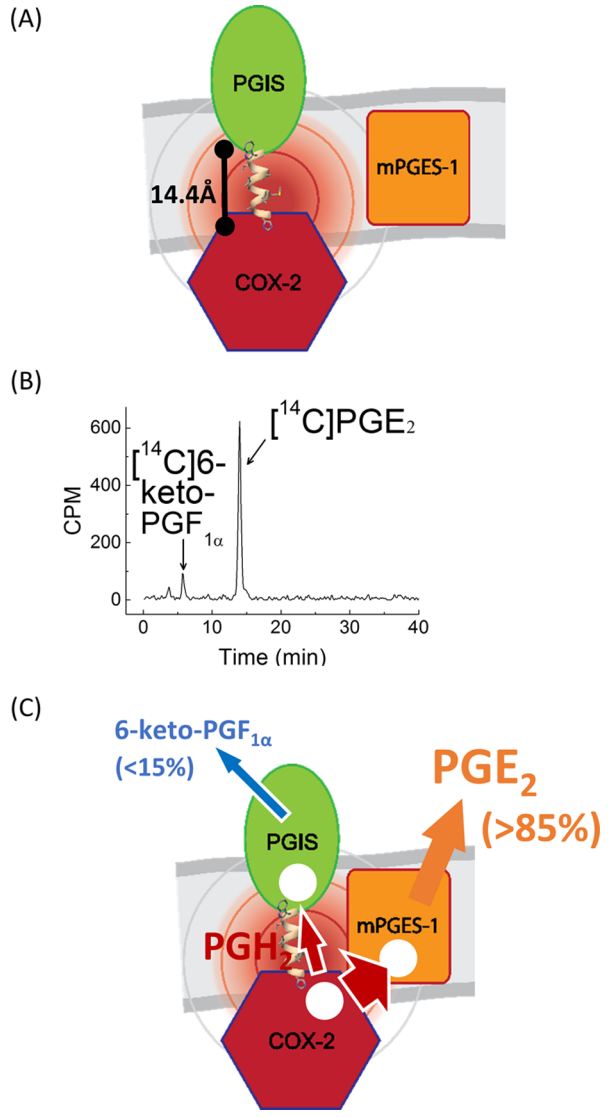

Figure 4. (A) Competition for COX-2-derived PGH2 between PGIS and mPGES-1. (B) Full profile of the incorporated [^{14}C]AA metabolite made by the HEK293 cells expressing COX-2, PGIS, and mPGES-1. (C) Putative models of the relationship between PGI2 synthesis and the distance between COX-2 and PGIS.

also indicated that the non-inflammatory COX-1-10aa-PGIS was not able to form a <14.4 Å contact with mPGES-1 in the ER membrane like COX-2-10aa-PGIS could (Figure 5C). This model explains why the inflammatory tissue requires COX-2 to produce PGE_2, but not COX-1.

Testing the Effect of Distance on mPGES-1 To Catch PGH_2 from COX-2-10aa-PGIS Using Separated ER Membranes. Finally, we mixed the separately expressed COX-2-10aa-PGIS[9] and mPGES-1 (Figure 1A, lane 3) using two different ER membranes of the cells. AA metabolites were monitored under the condition of the mixture of the one ER membrane-bound COX-2-10aa-PGIS and another ER membrane-bound mPGES-1. Under this condition, the separated mPGES-1 and COX-2-10aa-PGIS in the ER had no chance to express within a complexlike distance (Figure 6A). The AA metabolite assay showed that the majority of PGH_2 from the COX-2 domain was converted to PGI_2 by the PGIS domain within the fusion enzyme, and very little reached mPGES-1 in another ER membrane to produce PGE_2 (Figure 6B,C).

DOI: 10.1021/acs.biochem.5b00339
Biochemistry 2015, 54, 3707−3715

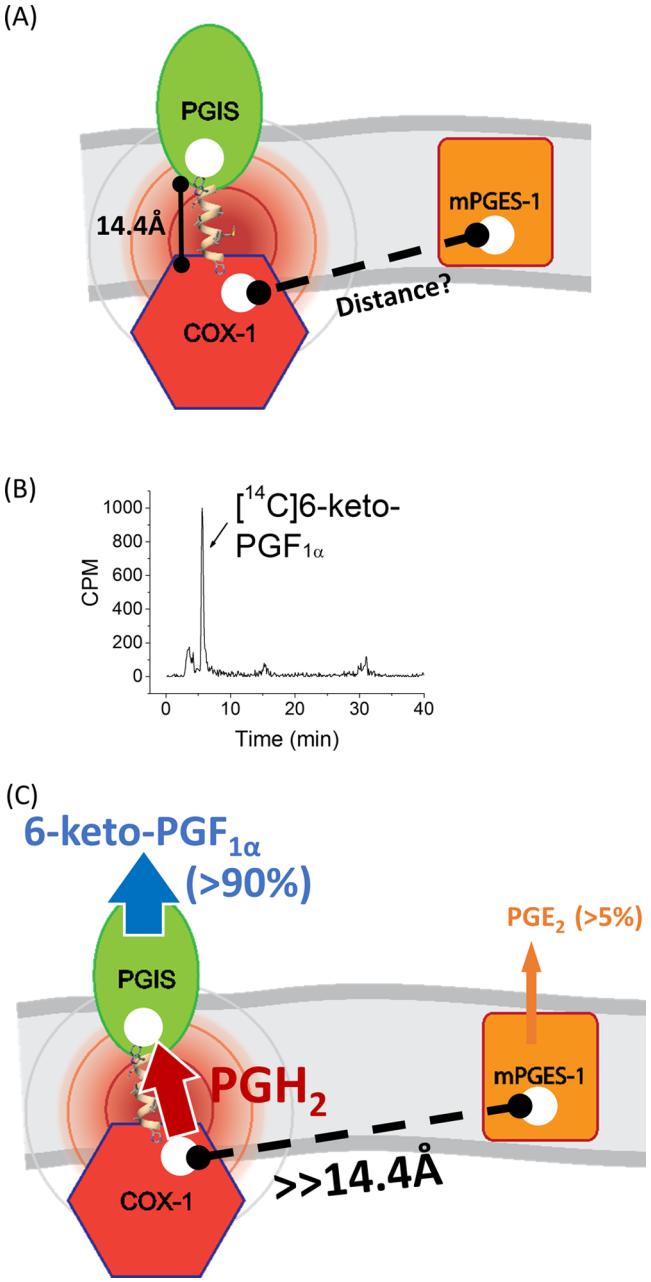

Figure 5. (A) Competition for COX-1-derived PGH2 between PGIS and mPGES-1. (B) Full profile of the incorporated [^{14}C]AA metabolite made by the HEK293 cells expressing COX-1, PGIS, and mPGES-1. (C) Putative model of the topological relationship among COX-1, PGIS, and mPGES-1.

DISCUSSION

In a pure enzyme assay, mPGES-1 can accept PGH_2 as a substrate from both COX-1 and COX-2. However, *in vivo*, the cellular inflammation mediated by pathogenic PGE_2 is produced selectively by mPGES-1 accepting PGH_2 from inducible COX-2, but not COX-1. So far, the molecular and cellular mechanisms are little known. However, understanding the mechanism for the selectivity is a key step in uncovering the inflammatory process and its relative cardiovascular diseases and cancers. There are several possibilities to be considered for the selectivity, including that a larger amount of PGH_2 was produced by COX-2 than by COX-1 in the cells, that the expression level of COX-2 is higher than that of COX-1 in the inflammatory cells, or that the molecule−molecule interaction in ER bilayers favors COX-2 coordinated with mPGES-1 more than that of COX-1. We used the designed fusion enzymes with 1:1 stoichiometry of COX-2 or COX-1 with PGIS (COX-2-10aa-PGIS or COX-1-10aa-PGIS, respectively) to analyze AA metabolites. These stoichiometric designs allow us to precisely determine how much PGH_2 generated by one molecule of COX enzyme is passed to one molecule of PGIS in the ER membrane inside the cells. In these cases, the amounts of PGH_2 produced by COX-1 and COX-2 domains passing to PGIS domains occurred at equal rates. Figure 4 showed PGH_2 produced by COX-2-10aa-PGIS was largely converted to PGE_2 in the presence of mPGES-1, but only a small amount of PGH_2 was converted to PGE_2 by COX-1-10aa-PGIS under the same condition (Figure 5). Therefore, the first and second possibilities explaining the differences of the PGH_2 concentration and expression levels can be excluded. Thus, the favorable protein−protein interaction between COX-2 and mPGES-1 hypothesized for the third possibility is likely a fundamental reason for the pathogenic PGE_2 production in the ER membrane during the inflammatory process.

In the past, most experiments used to study the protein−protein interaction in lipid bilayers included double staining of the co-expressed proteins,[9] the transfer of energy to predict their separation on the membrane,[10] measurement of the incorporated spin-labeled compound in the interested proteins in the membrane, and a protein crystallography approach to obtain images for the protein−protein interaction in purified forms. In this study, we have introduced an approach, "The Bioruler", using the active fusion enzymes (COX-2 or COX-1-linker-PGIS) with a well-defined interprotein distance as a "rule" to measure the enzymatic product, PGH_2, moved from one catalytic domain to another catalytic domain in a competitive manner. It was able to predict the unknown separation distance between COX-2 or COX-1 and mPGES-1 in the ER membrane (Figures 1−6). On the basis of the diffusion theory, the lipid molecule, PGH_2, freely diffuses in the ER membrane from COX-2 to the surrounding membrane proteins. The membrane-spanning mPGES-1 was able to catch PGH_2 from the COX-2 domain, and reduced PGH_2 diffused to the PGIS domain, which is 14.4 Å from the COX-2- or COX-1-10aa-PGIS fusion enzyme (Figures 3−5), which clearly demonstrates that the separation between the active sites of COX-2 and mPGES-1 is <14.4 Å. Via replacement of COX-2-10aa-PGIS with COX-1-10aa-PGIS, mPGES-1 lost the priority to catch PGH_2 from the COX-1 domain and let PGH_2 move to the PGIS domain, converting to PGI_2 (Figure 4). This demonstrates that mPGES-1 is much more than 14.4 Å from the COX-1 domain on the ER arrangement (Figure 5). It led us to conclude that the selectivity of mPGES-1 accepting PGH_2 from COX-2 is caused by the complexlike protein−protein arrangement (within ≤14.4 Å) of COX-2 and mPGES-1 on the ER lipid bilayers. Thus, it also led us to speculate that during the inflammatory stimulation, because the expressed COX-2 and mPGES-1 are folded into 3D structures and anchor to the ER membrane, they have to form a complexlike colocalization in the ER membrane to make a large amount of pathogenic PGE_2 (Figure 7A). In contrast, the expressed COX-1 is not organized into a complexlike colocalization with mPGES-1 (Figure 7B). The factors attracting COX-2 and mPGES-1 together to organize into a complexlike intermolecular distance could be another challenging issue to be solved. This is the first report providing evidence showing the effects of the

DOI: 10.1021/acs.biochem.5b00339
Biochemistry 2015, 54, 3707−3715

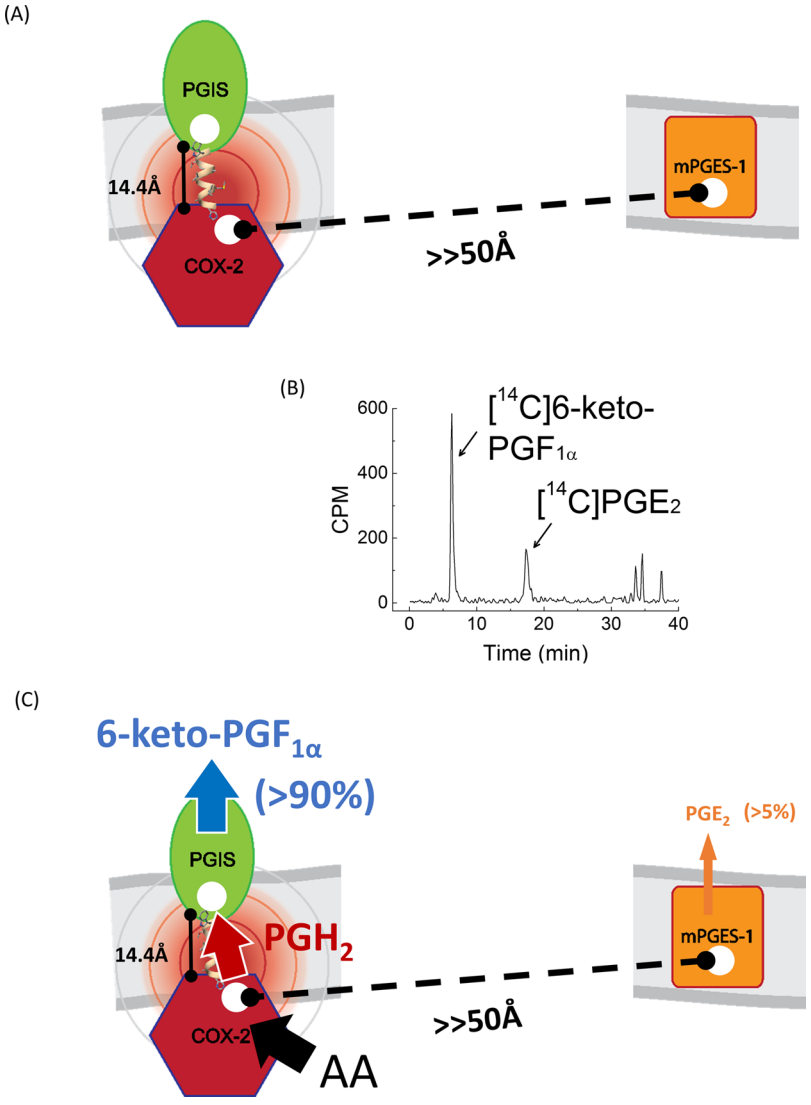

Figure 6. (A) Competition for COX-2-derived PGH2 between PGIS in the same cell and mPGES-1 in a different cell. (B) Full profile of the incorporated [^{14}C]AA metabolite made by the mixture of the separately expressed COX-2-10aa-PGIS and mPGES-1 in two different ER membranes of the cells. (C) Putative model of the topological relationship between PGIS in the same cell and mPGES-1 in a different cell.

postexpression arrangement of COX-2 and mPGES-1 in the ER lipid bilayer on the pathological PGE_2 biosynthesis, and the differences in the ER arrangements between COX-2 and COX-1 (Figure 7).

This finding has also provided more detailed insights into why mPGES-1 knockout mice redirecting AA from PGE_2 to other metabolites are resistant to inflammation observed previously. In inflammatory factor-induced macrophages isolated from wild-type mice, AA was metabolized to prostanoids in the following order: PGE_2 > TXB_2 > 6-keto-$PGF_{1\alpha}$ and $PGF_{2\alpha}$. In contrast, the order was redirected to the following in the macrophages isolated from mPGES-1 knockout mice: TXB_2 > 6-keto-$PGF_{1\alpha}$ and $PGF_{2\alpha}$ > PGE_2.[14] The molecular mechanism was not clearly addressed before. The study presented here, identifying the distance between inducible COX-2 and mPGES-1 on the ER membrane that is shorter than that between mPGES-2 and cPGES, allowed us to develop a hypothesis regarding the molecular and cellular mechanisms. When inflammation occurred *in vivo*, PGH_2 metabolized from AA by the induced COX-2 is immediately diffused to mPGES-1, which is closer to COX-2 compared to that of other downstream PG enzymes, mPGES-2, and cPGES. PGH_2 is then converted into a high level of inflammatory PGE_2. In the mPGES-1 knockout mice, mPGES-2 and cPGES are not close enough to COX-2 to catch COX-2-derived PGH_2, which results in a 95% reduction in the level of PGE_2 biosynthesis, and redirects AA metabolites in a different order described above in the cells. Understanding the molecular and cellular mechanisms for the redirected AA metabolites helps us understand how the mPGES-1 knockout mice resist the induction of inflammation. In addition, passing the COX-produced PGH_2 to the specific downstream synthase to produce particular prostanoids from AA is a common step and involved directly in controlling many pathophysiological processes, including vascular, blood coagulation, and heart diseases, cancer development, asthma symptoms, and reproductive diseases. A recent study using COX-2 and mPGES-1 knockout mice has indicated that the PGE_2 synthesized by inflammatory factor-induced COX-2 and mPGES-1 in brain endothelial cells is a major prostaglandin and critical to inflammation.[15] It has led us to predict that our finding using the recombinant cells might be applied to the endothelial cells.

DOI: 10.1021/acs.biochem.5b00339
Biochemistry 2015, 54, 3707−3715

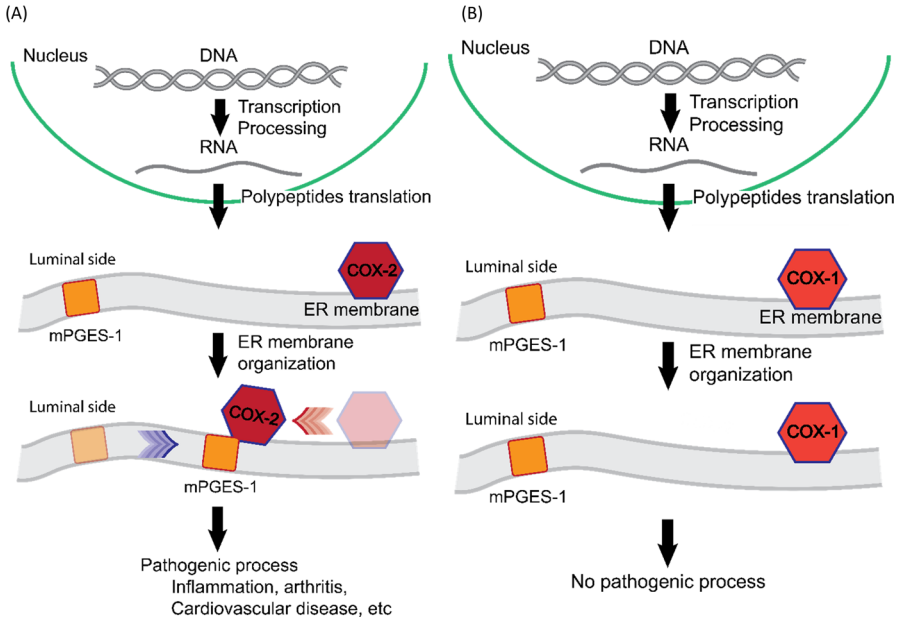

Figure 7. Proposed post-translational ER organization of COX-2 and mPGES-1 (left) and COX-1 and mPGES-1 (right). COX-2 and mPGES-1 form a complexlike contact in the ER membrane (left). The expressed COX-1 is not organized into a complexlike contact with mPGES-1 (right).

This could be useful to improve our understanding of the pathophysiological processes of inflammatory diseases mediated by endothelial dysfunction.

■ CONCLUSIONS

This study has demonstrated that the protein−protein arrangement of COXs and their downstream enzymes are the key steps in the specific PGE_2 biosynthesis to control the pathophysiological processes in cells. "The Bioruler", fusion enzymes of COX-1 or COX-2 linked to PGIS with defined 14.4 and 30.8 Å (10 and 22 aa) distances, could also be used as references to measure the distances between the COXs and other downstream synthases such as TXAS, PGFS, PGDS, mPGES-2, and cPGES in live cells by monitoring the movement of COXs-derived PGH_2 to be metabolized to the corresponding prostanoids. Thus, this study has provided a new tool for improving our understanding of the interaction of COXs with their downstream synthases in live cells and helps uncover the pathophysiological process, which are mediated by the corresponding prostanoids.

■ AUTHOR INFORMATION

Corresponding Author

*Department of Pharmacological and Pharmaceutical Sciences, Center for Experimental Therapeutics and Pharmacoinformatics, College of Pharmacy, University of Houston, 552 Science and Research Building 2, 4800 Calhoun Rd., Houston, TX 77204-5037. E-mail: khruan@uh.edu. Phone: (713) 743-1771. Fax: (713) 743-1229.

Author Contributions

We take responsibility for all aspects of the reliability and freedom from bias of the data presented and their discussed interpretation.

Funding

This study was supported by National Institutes of Health Grants R01HL056712, R01HL079389, R01HL056712-11S1 and R01HL056712-13S1, U.S. Army Grant W81XWH-10-2-0125, and American Heart Association Grants 10GRNT4470042 and 14GRNT20380687 (to K.-H.R.).

Notes

The authors declare no competing financial interest.

■ ACKNOWLEDGMENTS

We thank Xiaoyin Tan for assistance with manuscript preparation.

■ ABBREVIATIONS

PGE_2, prostaglandin E_2; mPGES-1, microsomal PGE_2 synthase-1; PGI_2, prostacyclin; PGIS, PGI_2 synthase; COX-1 and -2, cyclooxygenase-1 and -2, respectively; PGH_2, prostaglandin H2; AA, arachidonic acid; PGS, prostaglandin synthase; PGD_2, prostaglandin D2; PGF_2, prostaglandin F2; TXA_2, thromboxane A2; cPGES, cytosolic PGE_2 synthase; mPGES-2, microsomal PGES-2; ER, endoplasmic reticulum; TM, transmembrane; PGG_2, prostaglandin G2; aa, amino acid; HPLC, high-performance liquid chromatography; HEK293, human embryonic kidney 293.

■ REFERENCES

(1) Ricciotti, E., and FitzGerald, G. A. (2011) Prostaglandins and inflammation. *Arterioscler., Thromb., Vasc. Biol. 31*, 986−1000.

(2) Dorris, S. L., and Peebles, R. S. (2012) PGI2 as a Regulator of Inflammatory Diseases. *Mediators Inflammation 2012*, 1−9.

(3) Murakami, M., Nakatani, Y., Tanioka, T., and Kudo, I. (2002) Prostaglandin E synthase. *Prostaglandins Other Lipid Mediators 68−69*, 383−399.

(4) Caughey, G. E., Cleland, L. G., Penglis, P. S., Gamble, J. R., and James, M. J. (2001) Roles of Cyclooxygenase (COX)-1 and COX-2 in Prostanoid Production by Human Endothelial Cells: Selective Up-Regulation of Prostacyclin Synthesis by COX-2. *J. Immunol. 167*, 2831−2838.

(5) Camacho, M., et al. (2007) Microsomal prostaglandin E synthase-1, which is not coupled to a particular cyclooxygenase isoenzyme, is essential for prostaglandin E2 biosynthesis in vascular smooth muscle cells. *J. Thromb. Haemostasis 5*, 1411−1419.

DOI: 10.1021/acs.biochem.5b00339
Biochemistry 2015, 54, 3707−3715

(6) Hara, S., et al. (1994) Isolation and molecular cloning of prostacyclin synthase from bovine endothelial cells. *J. Biol. Chem. 269*, 19897−19903.
(7) Lin, Y., Wu, K. K., and Ruan, K. H. (1998) Characterization of the secondary structure and membrane interaction of the putative membrane anchor domains of prostaglandin I2 synthase and cytochrome P450 2C1. *Arch. Biochem. Biophys. 352*, 78−84.
(8) Penglis, P. S., Cleland, L. G., Demasi, M., Caughey, G. E., and James, M. J. (2000) Differential regulation of prostaglandin E2 and thromboxane A2 production in human monocytes: Implications for the use of cyclooxygenase inhibitors. *J. Immunol. 165*, 1605−1611.
(9) Ruan, K. H., Deng, H., and So, S. P. (2006) Engineering of a protein with cyclooxygenase and prostacyclin synthase activities that converts arachidonic acid to prostacyclin. *Biochemistry 45*, 14003−14011.
(10) Ruan, C. H., So, S. P., and Ruan, K. H. (2011) Inducible COX-2 dominates over COX-1 in prostacyclin biosynthesis: Mechanisms of COX-2 inhibitor risk to heart disease. *Life Sci. 88*, 24−30.
(11) Hanaka, H., et al. (2009) Microsomal prostaglandin E synthase 1 determines tumor growth in vivo of prostate and lung cancer cells. *Proc. Natl. Acad. Sci. U.S.A. 106*, 18757−18762.
(12) Nithipatikom, K., et al. (2002) Requirement of cyclooxygenase-2 expression and prostaglandins for human prostate cancer cell invasion. *Clin. Exp. Metastasis 19*, 593−601.
(13) Ruan, K. H., Cervantes, V., and So, S. P. (2009) Engineering of a novel hybrid enzyme: An anti-inflammatory drug target with triple catalytic activities directly converting arachidonic acid into the inflammatory prostaglandin E2. *Protein Eng., Des. Sel. 22*, 733−740.
(14) Trebino, C. E., et al. (2005) Redirection of eicosanoid metabolism in mPGES-1-deficient macrophages. *J. Biol. Chem. 280*, 16579−16585.
(15) Wilhelms, D. B., et al. (2014) Deletion of Prostaglandin E2 Synthesizing Enzymes in Brain Endothelial Cells Attenuates Inflammatory Fever. *J. Neurosci. 34*, 11684−11690.

DOI: 10.1021/acs.biochem.5b00339
Biochemistry 2015, 54, 3707−3715